# Design and implementation of an infrared plenoptic camera

Kevin Cossu, Guillaume Druart, Mathieu Chambon, Eric Belhaire, Frédéric Champagnat, Thierry Lépine

# DESIGN AND IMPLEMENTATION OF AN INFRARED PLENOPTIC CAMERA

**Kevin Cossu [1,2,3], Guillaume Druart [2], Mathieu Chambon [2], Eric Belhaire [1], Frédéric Champagnat [2], Thierry Lépine [3]**

*[1] Thales Optronique SA, 2 Avenue Gay Lussac, 78990 Elancourt, France*
*[2] ONERA, Chemin de la Hunière, 91123 Palaiseau Cedex, France*
*[3] CNRS UMR 5516, Laboratoire Hubert Curien and Institut d'Optique, 18 Rue Professeur Benoît Lauras, 42000 Saint-Etienne, France*
*Corresponding author: kevin.cossu@fr.thalesgroup.com*

**KEYWORDS:** Infrared, Plenoptic camera, Lightfield, Microlens array, Optical design.

**ABSTRACT:**

Huge efforts have been made over the past years to miniaturize cameras working in the visible spectrum and to give them new features. Plenoptic cameras for example have emerged as a new way of capturing more than just a single 2D image. These cameras usually include a microlens array positioned between the main lens of the camera and the sensor such that a point in object space is imaged onto multiple pixels. This allows for single snapshot image refocusing or depth estimation. The need for more features in a limited volume is also critical in the military domain. However, defense applications usually require the use of sensors that work in the non-visible spectrum such as cooled infrared sensors. This brings an additional challenge to the design of compact and functionalized cameras. In this paper we explain how we overcame these constraints to design and implement the first cooled infrared plenoptic camera and demonstrate its imaging and distance estimation capabilities.

## 1. INTRODUCTION

Cameras in the visible region have seen some dramatic improvements over the past years. The rapid growth of the smartphone market has led the camera manufacturers to increase their performance on every aspect including megapixel count, noise, crosstalk between pixels or high dynamic range. Today, these evolutions have reached a certain limit as it is more difficult to assess the improvements they bring. That is why we see a growing interest for new features like 3D imaging.

High performance infrared sensors are also improving over the years, especially regarding two aspects that are the pixel size and the total number of pixels on each sensor. But the pixel size in infrared sensors is about one order of magnitude higher than in visible sensors mainly due to the hybridization process involved in the manufacturing of these sensors. That is why today's standard infrared sensors only include about 1 million pixels. However this number of pixel is now sufficient to obtain very sharp images. It is therefore an appropriate time to follow what is being done in the visible region and consider adding more features to infrared cameras. Here we describe a way to give a depth estimation capabilitiy to an infrared camera through plenoptic imaging.

## 2. INFRARED SENSORS

Infrared cameras (or thermal cameras) operate in the Mid-Wavelength Infrared (MWIR) between 3µm and 5µm or the Long-Wavelength Infrared (LWIR) between 8µm and 12µm. They are capable of producing images of the same quality during both day and night, and can, in certain conditions, see through mist or smoke. These high performance infrared cameras are also very expensive, which is why they were mostly used for defense or surveillance applications. It is however noteworthy to mention that cheap uncooled infrared sensors with lower

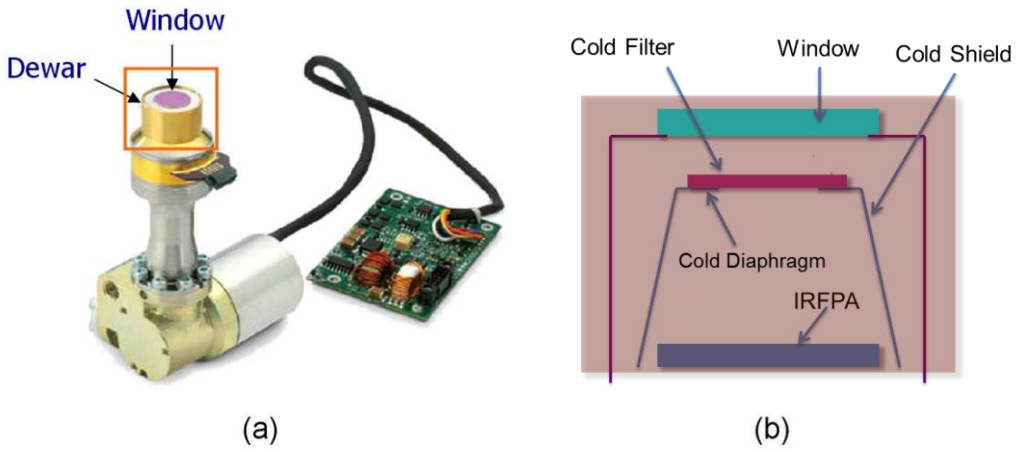


*Figure 1 – (a) External view of a Dewar commercialized by Sofradir. (b) Internal view of a Dewar*

performance aimed at lower-cost applications are emerging rapidly. In this paper we will only consider the former type of high performance cooled infrared sensors.

These sensors need to be embedded in a sealed, cooled cryogenic environment called a dewar. The dewar typically includes a window, a cold shield and a cold diaphragm to limit the sensor's field of view as shown in Fig. 1.

The fact that high performance infrared cameras require the use of a dewar brings many challenges to the optical design of these cameras. Indeed, the dewar being a closed environment and its typical height being around 20mm implied that no lens could be put near the infrared focal plane array (IRFPA). The integration of optics directly inside the dewar was recently proposed [1] to overcome this constraint. This way, the optics are cooled down to a known temperature, thus tackling many issues such as, for example, the size of the camera or the need for athermalization.

One should however keep in mind that adding optical elements inside the dewar increases the total mass that needs to be cooled down and thus the time that it takes for the system to be operational. Furthermore the dimensions of the cold shield are small.

Bringing 3D vision to a device usually means adding more cameras or adding active lighting elements such as pulsed laser sources to an already constrained space. For example in the case of micro air vehicles that are very constrained both in terms of size and weight, it may not be possible to add more equipments to the payload. Furthermore, high performance infrared cameras or lasers are very expensive so the option of multiplying them will usually not be available.

That is why we decided to design an infrared camera that could allow 3D imaging with a single camera such as the plenoptic camera.

## 3. THE PLENOPTIC CAMERA

First proposed in 1908 by Gabriel Lippmann [2], the concept of integral photography really took off in 1992 with the introduction of the plenoptic camera [3] (or lightfield camera). The idea was to place a microlens array between the main lens and the sensor such that rays entering the camera would be focused by the main lens on the microlens array and be separated by it over multiple pixels on the sensor (see Fig. 2). That way, a single point in object space is seen from several points of view on the different pixels behind a microlens, enabling features such as depth estimation or image refocusing.

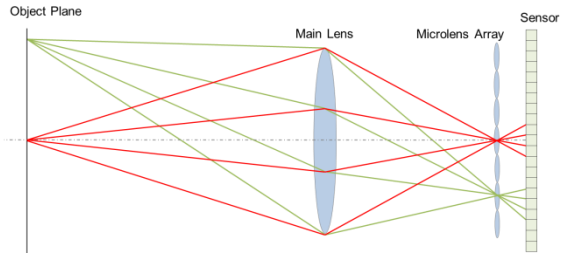


*Figure 2 - The plenoptic 1.0 camera: a single object point is seen by several pixels behind a single microlens.*

An improved version in terms of spatial resolution called plenoptic 2.0 was then introduced [4] in which the main lens does not focus rays on the microlens array but focuses instead in an intermediate plane which is then imaged by the microlenses onto the sensor (see Fig. 3).

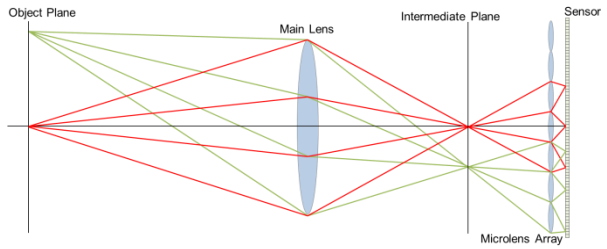


*Figure 3 – The plenoptic 2.0 camera: a single object point is imaged by the main lens in an intermediate plane and is seen by several microlenses. This configuration is called "real intermediate plane".*

The plenoptic camera is an ideal candidate for infrared 3D imaging because it is composed of two separate optical units, namely the main lens and the microlens array. This way, it can be transposed in the infrared region by integrating the microlens array in the dewar and leaving the main lens uncooled.

## 4. OPTICAL DESIGN

Each version of the plenoptic camera captures the lightfield in a different way. In the 1.0 case, the spatial resolution of a reconstructed image of the scene is given by the number of microlenses in the array. The angular resolution, which is directly linked to the depth we want to estimate, is given by the number of pixels behind each microlens. In the 2.0 case, both the spatial resolution and the angular resolution depend on the number of microlenses that form an image of the same object point on the sensor. This gives more flexibility to adjust the tradeoff between spatial and angular resolution. That is why, given the low pixel count of infrared sensors, we chose to design a plenoptic 2.0 camera. We will address the major steps of this design in the following subsections.

### 4.1. Configuration

There are two possible configurations for the plenoptic 2.0 camera: the real intermediate plane configuration and the virtual intermediate plane configuration.

In the real intermediate plane configuration, the main lens forms an image of the scene ahead of the microlenses (see Fig.3).

In the virtual intermediate plane configuration, the main lens forms an image of the scene behind of the microlenses (see Fig.4).

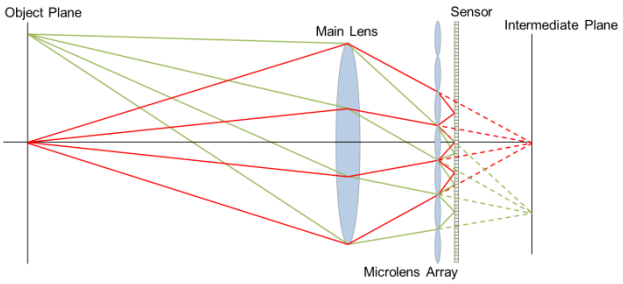


*Figure 4 – The plenoptic 2.0 camera in "virtual intermediate plane" configuration.*

There are two substantial differences between the real intermediate plane configuration and the virtual intermediate plane configuration. The first one lies in the way crosstalk between two sub-images is handled in both configurations. Indeed, better performance can be obtained with the real intermediate plane configuration for the same aperture of the main lens as detailed in [5]. The second difference is the fact that the virtual intermediate plane configuration has a shorter total track than the real intermediate configuration, thus minimizing the height of the cold shield. For this last reason, we selected a virtual intermediate plane configuration.

### 4.2. Multiview factor

The purpose of our camera is to capture a single image from which the depth of objects in the scene can be estimated. This estimation is directly linked to the disparity between two sub-images of the same object point. The accuracy of the depth estimation increases with the distance between the two microlenses considered for the disparity measurement. Thus, for a given microlens size, the more microlenses see a same object point, the better the precision of the depth estimation will be. We define the multiview factor $M_f$ as the number of microlenses that see a same object point

$$M_f = \frac{WF\#_{\mu L} * a/b}{WF\#_{ML}} \qquad (1)$$

Where ***WF#*** stands for "working F-number", ***µL*** stands for "microlens", ***ML*** stands for "main lens", ***a*** is the distance between the microlens array and the intermediate plane and ***b*** is the distance between the microlens array and the Focal Plane Array. It is interesting to note that an object point will always be seen by at least N microlenses along one axis of the microlens array if $M_f$ is greater than N-1. This expression also shows that, for a given microlens array setup, the multiview factor increases with the aperture of the main lens.

However this increase in depth resolution comes at the cost of spatial resolution. In the case of infrared imaging, the low pixel count requires us to limit the number of microlenses that see a same object in order to keep an acceptable spatial resolution. We chose a multiview factor of 1.5 for our design.

### 4.3. Microlenses arrangement

Microlenses can be arranged with different shapes and patterns. We designed our system with circular microlenses rather than square microlenses in order to simplify the manufacturing process. Consequently, we chose a hexagonal pattern rather than a square pattern in order to minimize the number of "blind" pixels on the sensor, i.e. the number of pixels that do not belong to any sub-image.

## 5. PROTOTYPE

Based on the steps given in subsection 4, we designed and implemented the first infrared plenoptic camera. Our working prototype was designed to produce sharp images of objects located further than 0.8m from the camera. It is composed of a 25mm retrofocus objective coupled with a cooled microlens array integrated inside the dewar and a HgCdTe (also known as MCT) MWIR Focal Plane Array that has a pixel pitch of 15µm and VGA format. Our microlenses are made of Silicon and are arranged in an hexagonal array. We designed our system so that any point in its field of view is imaged by at least two microlenses along one axis of the microlens array. The complete optical block fits inside a 7cmx3cmx3cm volume.

### 5.1. Performance

#### 5.1.1 MTF

We measured the Modulation Transfer Function (MTF) of our camera using a Spot Scan method. This method works as follows: a black body illuminates a pinhole placed at the object focal plane of a collimator. The camera forms an image of the resulting point source on the sensor. Then we slightly rotate the camera, resulting in a sub-pixel horizontal (or vertical) shift of the image spot on the sensor and we repeat the process. This way we obtain a well-sampled Point Spread Function (PSF). The absolute value of the Fourier Transform of this PSF gives the MTF. We measured the MTF for several field angles in multiple microlenses and compare them to the MTF calculated with the optical design software Zemax. Fig. 5 shows the resulting theoretical and experimental MTF for different field angle inside a microlens.

From Fig. 5 we see that the camera behaves as predicted by Zemax inside a given microlens. We also note that the image quality be decays as we move away from the optical axis of our microlenses. This is a

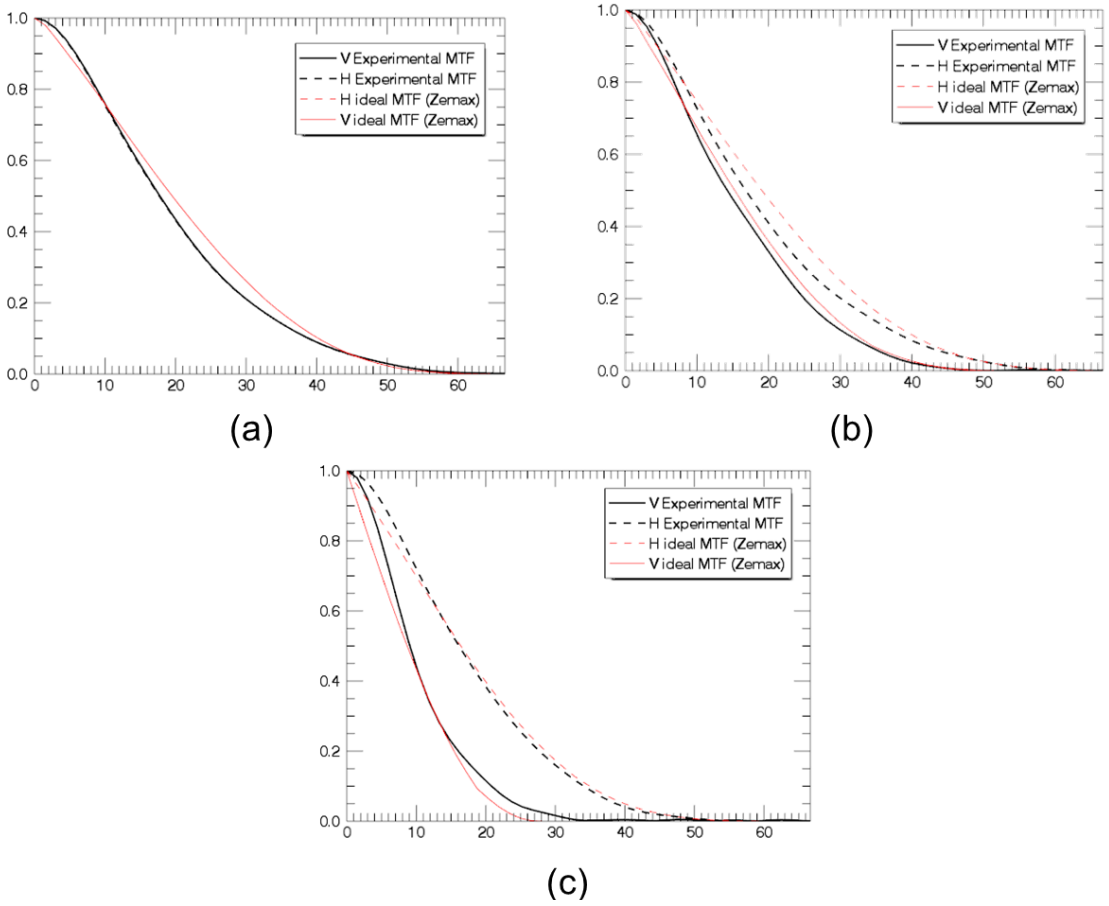


*Figure 5 – MTF plots for different field angles ($\theta$) inside the central microlens. Spatial frequencies along the horizontal axis are given in cycles/mm. (a) On axis, $\theta$=0°. (b) $\theta$=0.73°. (c) $\theta$=1.17°*

consequence of the vignetting of our microlenses. Indeed, whereas vignetting is known for improving the image quality in standard camera by blocking marginal rays, it has the opposite effect in the case of the plenoptic 2.0 camera. Fig. 6 illustrates this phenomenon: in a given sub-image, rays that hit the center of the sub-image come from the center portion of the pupil of the main lens, resulting in good image quality. However as we move further from the center of the sub-image, rays that hit the sensor come from more peripheral portions of the pupil of the main lens, thus resulting in lower image quality.

Fig. 7 shows the theoretical and experimental MTF measured at the center of various sub-images in the array. We see that the measured MTF fit the expected result and that the image quality does not vary between different microlenses in the array.

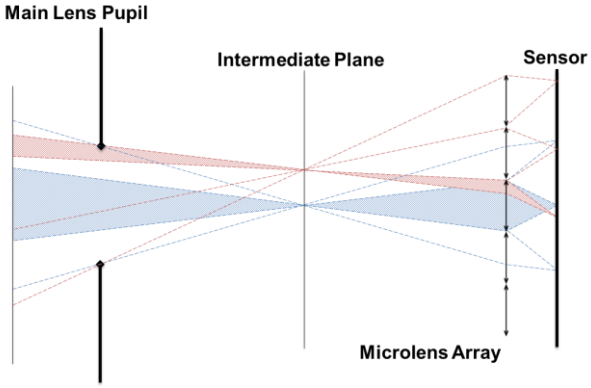


*Figure 6 – Impact of the vignetting of the microlenses on the image quality. The blue fan of rays passes through the center of the main lens pupil whereas the red fan of rays passes through a peripheral portion of the main lens pupil. A real intermediate plane configuration was chosen for simplicity purposes.*

### 5.1.2 Depth Estimation Capability

Our camera has a depth of field ranging from 0.8m to infinity. two sub-images of a same object point will be spaced by a value that is proportional to the distance of that object from the camera. Assuming tenth of a pixel, state of

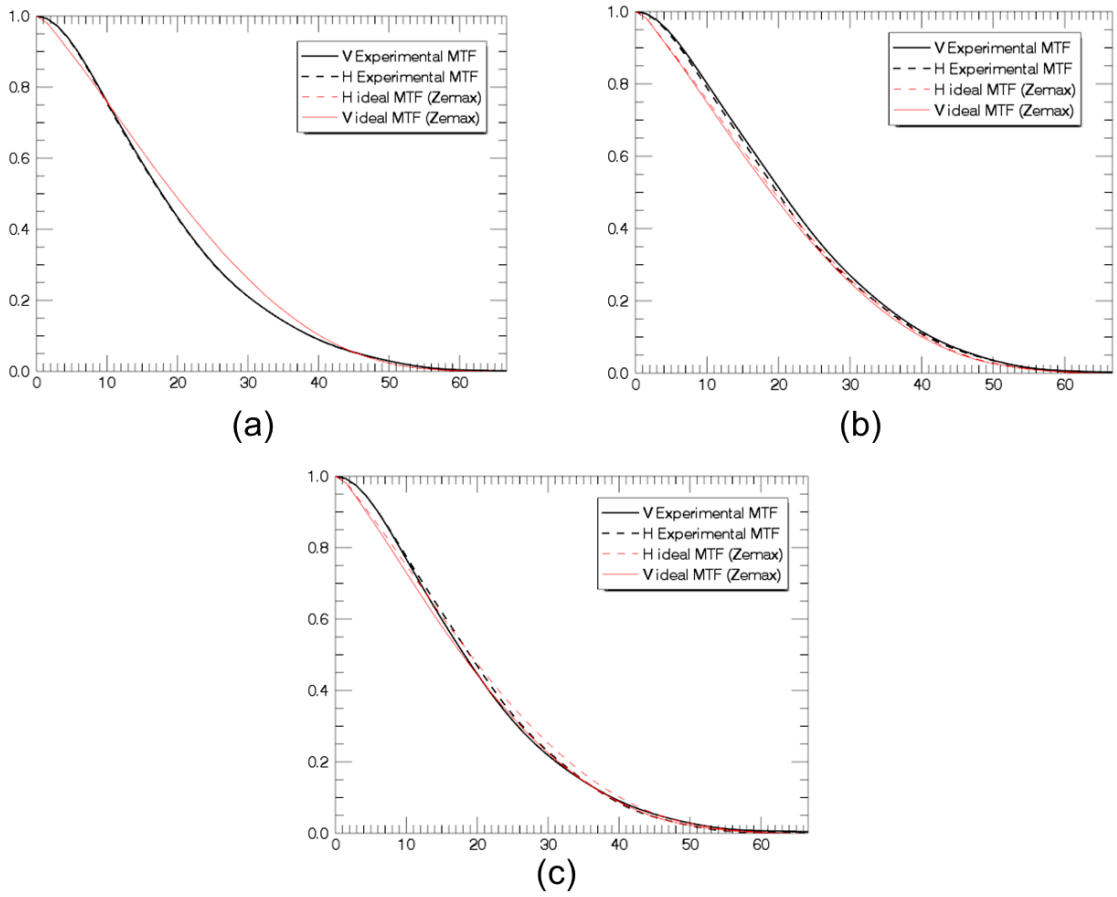


*Figure 7 – On axis MTF plots for different microlenses in the array. Spatial frequencies along the horizontal axis are given in cycles/mm. (a) On axis, $\theta$=0°. (b) $\theta$=8°. (c) $\theta$=11°*

the art accuracy on the estimation of the disparity, we find that our camera can distinguish 14 different object planes within its depth of field. We have verified this experimentally. More details will be given in future papers.

### 5.2. Images

The images shown in Fig. 8 were taken with our prototype and processed to obtain "non-plenoptic images" as the ones shown in Fig. 9. These reconstructed images were assembled from small patches taken in each sub-image of the plenoptic images. Note that other techniques can be used to obtain reconstructed images such as backward propagation [6]. Furthermore, the resolution can be enhanced with by using super-resolution algorithm [7].

## 6. CONCLUSION

In this paper, we present the design and implementation of a compact infrared plenoptic camera. We show images taken with a working prototype and illustrate its depth estimation capabilities. We have explained the challenges brought by this specific optical system and how we overcame these challenges. The prototype was designed to give depth information between 1 and 10 meters while maintaining an acceptable spatial resolution. Work is in progress to further enhance this design and to adapt it to various applications.

## 7. ACKNOWLEDGEMENT

This work was sponsored by the Association Nationale de la Recherche et de la Technologie (ANRT) and the French Procurement Agency (DGA). We would also like to thank the CEA Leti for the integration of the microlens array inside the dewar.

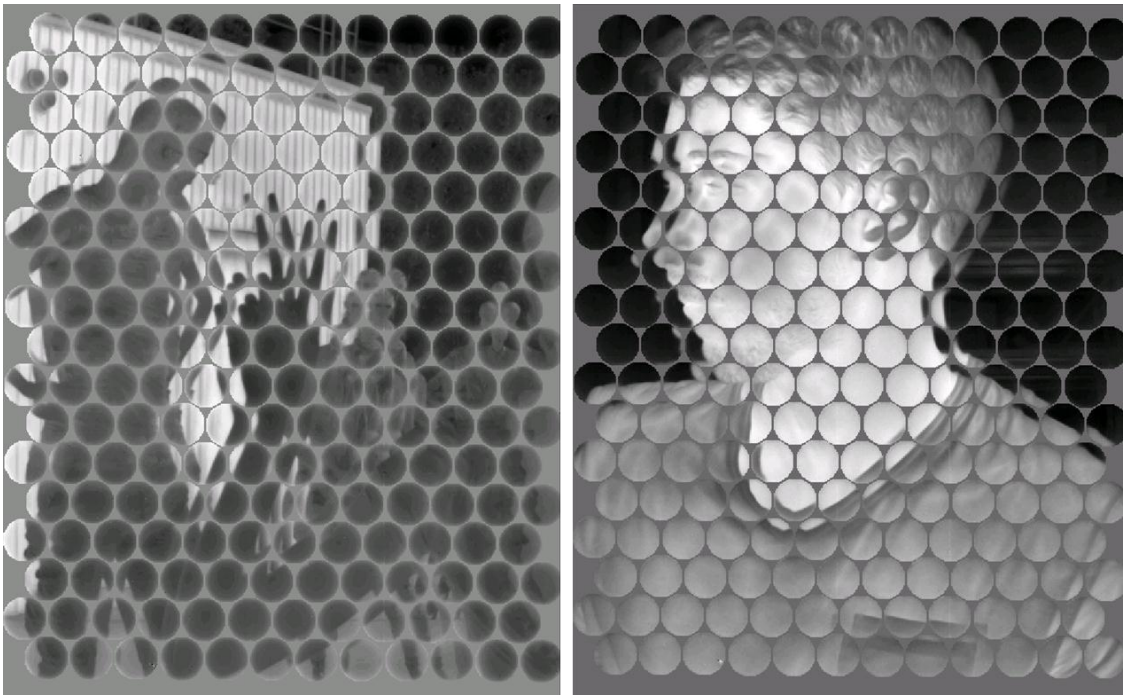

*Figure 8 – Images taken with our infrared plenoptic camera*

*Figure 9 – Non plenoptic image reconstructed from our plenoptic image*

## 8. REFERENCES


1. Druart G., Matallah N., Guérineau N., Magli S., Chambon M., Jenouvrier P., Mallet E., Reibel Y. (2014). OSMOSIS : a new joint laboratory between SOFRADIR and ONERA,for the developement of advanced DDCA with integrated optics. *Proc. SPIE 9070.*
2. Lippman G. (1908). Epreuves réversibles, photographie intégrale. *Comptes Rendus de l'Académie des Sciences de Paris 146, p.446 à 451*
3. Adelson E.H., Wang J. (1992). Single lens stereo with a plenoptic camera. *PAMI 14(2), 99–106*

4. Lumsdaine A., Georgiev T. (2008). Full resolution lightfield rendering, *Technical Report, Adobe Systems, Inc.*

5. Cossu K., Druart G., Chambon M., Belhaire E., Champagnat F., Lépine T. (2016). Crosstalk reduction in the plenoptic camera. *10th International Conference on Optics-photonics Design and Fabrication.*

6. Sommer H., Ihrig. A, Ebenau M., Flühs D., Spaan B., Eichmann M. (2014). Integral image rendering procedure for aberration correction an size measurement. *Appl. Opt. 53, 3176-3182.*

7. Georgiev T., Lumsdaine A. (2009). Superresolution with plenoptic 2.0 cameras. *Frontiers in Optics 2009, OSA Technical Digest, paper STuA6.*